Progress In Electromagnetics Research, Vol. 127, 277–295, 2012

EFFICIENT MODEL ORDER REDUCTION FOR FEM ANALYSIS OF WAVEGUIDE STRUCTURES AND RESONATORS

G. Fotyga*, K. Nyka, and M. Mrozowski

Faculty of Electronics, Telecommunications and Informatics, Gdansk University of Technology, 11/12, G. Narutowicza St., Gdansk 80-233, Poland

Abstract—An efficient model order reduction method for three-dimensional Finite Element Method (FEM) analysis of waveguide structures is proposed. The method is based on the Efficient Modal Order Reduction (ENOR) algorithm for creating macro-elements in cascaded subdomains. The resulting macro-elements are represented by very compact submatrices, leading to significant reduction of the overall number of unknowns. The efficiency of the model order reduction is enhanced by projecting fields at the boundaries of macro-elements onto a subspace spanned by a few low-order waveguide modes. The combination of these two techniques results in considerable saving in overall computational time and memory requirement. An additional advantage of the presented method is that the reduced-order system matrix remains frequency-independent, which allows for very fast frequency sweeping and efficient calculation of resonant frequencies. Several numerical examples for driven and eigenvalue problems demonstrate the performance of the proposed methodology in terms of accuracy, memory usage and simulation time.

1. INTRODUCTION

Due to the growing demand for efficient and accurate microwave circuit simulation tools, model order reduction (MOR) techniques have recently received considerable attention in computational electromagnetics. The fundamental idea of MOR, developed originally in context of Linear Time Invariant dynamical systems, is to replace the

Received 16 February 2012, Accepted 21 March 2012, Scheduled 16 April 2012

* Corresponding author: Grzegorz Fotyga (grzegorz.fotyga@eti.pg.gda.pl).

original large set of state-space equations with a much smaller one in such a way, that the transfer function derived from the resultant system still provides satisfactory accuracy. Owing to significant decrease in the number of unknowns, the main benefit arising from this operation is the acceleration of computations, as well as the reduction of memory demand.

Developed over a decade ago, techniques of reduced-order modeling of large linear [1–3] and nonlinear [4] electronic circuits paved the way for applications of MOR in analysis of electromagnetic fields. Compact Padé approximation of the transfer functions of 3-D electromagnetic systems in FDTD method, via Lanczos (PVL) and PRIMA [2] algorithms, was proposed in [5]. This approach, along with an alternative one based on ENOR algorithm [6], evolved into the concept of macromodels (or macro-elements). They are generated by applying model order reduction locally in selected subdomains that require strong mesh refinement. The efficiency of the macromodeling technique was demonstrated for finite difference methods in time or frequency domain [6–8], as well as for the finite element method [9–11].

The idea of compact macromodels or macro-elements embedded in the analyzed structure was generalized to the form that serves as a tool for indirect domain decomposition [12, 13]. The entire computational domain can be divided into many subdomains, which are thereafter subject to independent model order reduction. Afterwards, the global structure is reassembled from the reduced subdomains as a matrix comprising coupled submatrices of macromodels [14, 15] or as a network of subcomponents described by generalized admittance matrices [13]. There is a significant difference between these two approaches. The former leaves the system matrix entries frequency-independent, while in the latter approach, the system matrix entries become a non-linear function of frequency.

Numerous efficiency enhancements of MOR techniques have recently been proposed for various applications, e.g., low-frequency response of multi-conductor transmission lines [16], ultra wideband systems such as UWB antenna [17], or PEEC modeling using multi-point moment matching technique [18].

This paper addresses the problem of applying model order reduction locally via macro-elements in a three-dimensional finite element analysis of waveguide structures and resonators. It is based on the general idea presented in [10], where 2-D scalar FEM method and macro-elements reduced by the ENOR algorithm [3] were used. In this reduction technique, selected parts of FEM matrices are compressed one by one by projecting their relevant blocks onto a subspace spanned

by an orthonormal basis, which is generated by the ENOR algorithm for one, arbitrarily chosen frequency. Unlike in the method using the PRIMA algorithm and the generalized admittance matrix [9, 13], the resulting system matrices remain frequency-independent. This is an important distinguishing feature of our approach, which implies two fundamental advantages: it is sufficient to make the reduction only once for wide frequency sweeps and, moreover, this approach can be employed in eigenvalue problems in order to allow for their solving solely, by means of standard techniques. So far we have demonstrated the application of the new type of frequency-independent macro-elements in 2-D FEM [10]. A direct extension of the 2-D method to the 3-D analysis requires introducing 3-D vectorial FEM formulation. This step is rather straightforward, however, the size of the macro-elements in 3-D grows very rapidly, which may lead to efficiency issues in some cases. It is caused by the fact that the computational cost of the reduction is dependent on two factors: the size of the macro-element (which is a product of the reduction order) and the size of the macro-element port (equal to the number of degrees of freedom of the mesh at the macro-element boundary). Unlike in the 2-D case where the size of 1-D macro-element boundary can be decreased to a very small number of nodes by proper mesh coarsening, in 3-D problems the number of elements at the 2-D boundary mesh is much bigger and usually significantly affects the reduction performance. Geometrical coarsening practically does not alleviate this problem, because a good quality 3-D mesh requires large space for gradual decrease in the mesh density within the macro-element regions.

In this paper we propose coarsening at macro-element ports by replacing large FEM basis with a much smaller one consisting of a few low-order modes. In other words, we decrease the size of an individual macro-element by projecting the fields of its boundary onto a subspace spanned by a reduced modal basis. A similar technique was used in [19] to interface subdomains of FEM and mode matching analysis. An alternative approach to modal decomposition and model order reduction in FEM analysis was proposed in [13]. However, the macromodels therein presented are based on generalized admittance matrix representation of each subdomain and involve a nonlinear function of frequency. The main advantage of our method is that no frequency-dependent terms occur in the matrices of macro-elements, thus enabling fast frequency sweeping in driven problems as well as efficient analysis of resonators. In this respect our approach follows the concepts presented in [20] for the FDTD method, and macromodels with intermediate projection on functional bases proposed in [15, 24] for finite-difference methods.

2. THEORY

2.1. Three-dimensional Finite Element Formulation

Consider a source-free bounded 3-D domain Ω. The electric field vector Helmholtz equation is:

$$\nabla \times \frac{1}{\mu_r} \nabla \times \vec{E} - k_0^2 \epsilon_r \vec{E} = 0 \tag{1}$$

where $\vec{E}$ is the electric field vector, $k_0^2 = \omega^2 \mu_0 \epsilon_0$ is the wavenumber, ω is the angular frequency, μ_0 and ϵ_0 are, respectively, the permittivity and permeability of the free space and μ_r, ϵ_r are the relative permittivity and permeability of the medium, respectively. The weak formulation of (1) is derived using the Galerkin method by multiplying the equation with the vector basis functions $\vec{w}$ and integrating the product over the computational domain Ω [22]:

$$\iiint_{\Omega} \nabla \times \vec{w} \cdot \frac{1}{\mu_r} \nabla \times \vec{E} dv + \iint_{\partial\Omega} \widehat{n} \times \frac{1}{\mu_r} \nabla \times \vec{E} \cdot \vec{w} ds - k_0^2 \iiint_{\Omega} \vec{w} \cdot \epsilon_r \vec{E} dv = 0 \tag{2}$$

where $\partial\Omega$ denotes the boundary of Ω, $\widehat{n}$ is the outward-pointing unit normal vector on $\partial\Omega$ [21, 22]. We assume the perfect electric conductor surface (PEC) on all physical walls, therefore the uniform Dirichlet boundary conditions are imposed on the tangential field components. The remaining parts of the boundary $\partial\Omega$ are regarded as ports of the structure, where the excitations are applied as nonuniform boundary conditions [13, 23]. Employing the FEM discretization of Ω using a tetrahedral mesh and the first-order basis functions, we obtain the following matrix equation:

$$\left(\mathbf{K} - k_0^2 \mathbf{M}\right) \mathbf{e} = \mathbf{b}, \tag{3}$$

which can be expressed as $\mathbf{Ge} = \mathbf{b}$. $\mathbf{K}$ and $\mathbf{M}$ are $N \times N$ sparse symmetric FEM matrices (stiffness matrix and mass matrix), N is the total number of variables, $\mathbf{e}$ — the vector of unknown coefficients of the FE basis functions associated with mesh edges, and $\mathbf{b}$ is the excitation vector. Once the Equation (3) has been solved, the reflection and transmission coefficients can be calculated.

2.2. Model Order Reduction Algorithm

First, we shall present extension of model order reduction procedure, proposed in [10] for 2-D, to 3-D vector problems. To this end a simple waveguide structure (Figure 1) is considered. The waveguide is terminated with two ports P_1, P_2, while the domain Ω is divided into

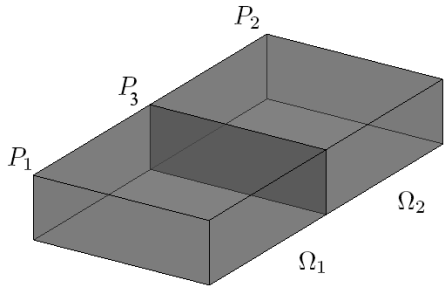

Figure 1. A basic waveguide structure divided into two subdomains: Ω_1 and Ω_2. Planes P_1, P_2 constitute external ports, while plane P_3 is an internal port.

two subdomains Ω_1 and Ω_2 by the interface P_3, henceforth referred to as an internal port. This is a model problem for a general class of 3-D waveguide structures and resonators divisible into many cascaded subdomains with transverse cross-section planes as interfaces. The most appropriate locations for those subdomains are regions which contain discontinuities, that require strong local mesh refinement. In practice the size of the subdomain is selected in such a way that its dimension does not exceed a wavelength at the center frequency. This limitation implies that the macro-element order is not too large. The internal ports should be placed in the uniform sections of the waveguide between discontinuities. Their placement is arbitrary, however, moving the ports closer to the discontinuities will increase the number of modes required in the modal projection, which is discussed in the Section 2.3.

If consistent numbering is used for the edges at ports P_1, P_2, P_3 and in subdomains Ω_1 and Ω_2, the matrices and vectors from (3) split into the following blocks:

$$\mathbf{K} = \begin{bmatrix} \mathbf{K}_{P1} & 0 & 0 & \mathbf{K}^T_{P1,\Omega1} & 0 \\ 0 & \mathbf{K}_{P2} & 0 & 0 & \mathbf{K}^T_{P2,\Omega2} \\ 0 & 0 & \mathbf{K}_{P3} & \mathbf{K}^T_{P3,\Omega1} & \mathbf{K}^T_{P3,\Omega2} \\ \mathbf{K}_{P1,\Omega1} & 0 & \mathbf{K}_{P3,\Omega1} & \mathbf{K}_{\Omega1} & 0 \\ 0 & \mathbf{K}_{P2,\Omega2} & \mathbf{K}_{P3,\Omega2} & 0 & \mathbf{K}_{\Omega2} \end{bmatrix}$$

$$\mathbf{M} = \begin{bmatrix} \mathbf{M}_{P1} & 0 & 0 & \mathbf{M}^T_{P1,\Omega1} & 0 \\ 0 & \mathbf{M}_{P2} & 0 & 0 & \mathbf{M}^T_{P2,\Omega2} \\ 0 & 0 & \mathbf{M}_{P3} & \mathbf{M}^T_{P3,\Omega1} & \mathbf{M}^T_{P3,\Omega2} \\ \mathbf{M}_{P1,\Omega1} & 0 & \mathbf{M}_{P3,\Omega1} & \mathbf{M}_{\Omega1} & 0 \\ 0 & \mathbf{M}_{P2,\Omega2} & \mathbf{M}_{P3,\Omega2} & 0 & \mathbf{M}_{\Omega2} \end{bmatrix}$$

$$\begin{aligned}\mathbf{e} &= \left[\begin{array}{ccccc} \mathbf{e}_{P1} & \mathbf{e}_{P2} & \mathbf{e}_{P3} & \mathbf{e}_{\Omega 1} & \mathbf{e}_{\Omega 2} \end{array}\right]^T \\ \mathbf{b} &= \left[\begin{array}{ccccc} \mathbf{b}_{P1} & \mathbf{b}_{P2} & 0 & 0 & 0 \end{array}\right]^T \end{aligned} \tag{4}$$

The first three rows and columns of $\mathbf{K}$ and $\mathbf{M}$ represent the elements located at the three ports of the structure (two external and one internal), whereas the last two rows and columns correspond to the two subdomains. The number of variables in each subvector of $\mathbf{e}$ is: N_{P1}, N_{P2}, N_{P3}, $N_{\Omega 1}$ and $N_{\Omega 2}$. The subscripts of the blocks outside of the main diagonal denote which subdomain is coupled with which port. Since it is assumed that excitation is imposed on the external ports, only the first two rows of the vector $\mathbf{b}$ are nonzero.

In order to compress Ω_1, Ω_2 into macro-elements by means of model order reduction (MOR) [10] using the ENOR algorithm [3], Equation (4) have to be transformed to the following form:

$$\left(\mathbf{C}s_0 + \Gamma\frac{1}{s_0}\right)\widehat{\mathbf{e}} = \mathbf{B}_e\mathbf{e}' \tag{5}$$

This represents the transfer function between the fields $\widehat{\mathbf{e}}$ (in a macro-element) and $\mathbf{e}'$ (elsewhere). After multiplication of (4) we obtain five equations, however only two of them are used in the reduction scheme, since there are only two subdomains:

$$\begin{aligned}&\left(\mathbf{K}_{P1,\Omega 1} - k_0^2\mathbf{M}_{P1,\Omega 1}\right)\mathbf{e}_{P1} + \left(\mathbf{K}_{P3,\Omega 1} - k_0^2\mathbf{M}_{P3,\Omega 1}\right)\mathbf{e}_{P3} \\ &+ \left(\mathbf{K}_{\Omega 1} - k_0^2\mathbf{M}_{\Omega 1}\right)\mathbf{e}_{\Omega 1} = 0 \end{aligned} \tag{6}$$

$$\begin{aligned}&\left(\mathbf{K}_{P2,\Omega 2} - k_0^2\mathbf{M}_{P2,\Omega 2}\right)\mathbf{e}_{P2} + \left(\mathbf{K}_{P3,\Omega 2} - k_0^2\mathbf{M}_{P3,\Omega 2}\right)\mathbf{e}_{P3} \\ &+ \left(\mathbf{K}_{\Omega 2} - k_0^2\mathbf{M}_{\Omega 2}\right)\mathbf{e}_{\Omega 2} = 0. \end{aligned} \tag{7}$$

After substituting:

$$\begin{aligned} s_0 = k_0, \quad \mathbf{C}_{\Omega 1} = \mathbf{M}_{\Omega 1}, \quad \Gamma_{\Omega 1} = -\mathbf{K}_{\Omega 1}, \\ \mathbf{B}_{\Omega 1} = \left[\frac{1}{s_0}\mathbf{K}_{P1,\Omega 1} - s_0\mathbf{M}_{P1,\Omega 1} \quad \frac{1}{s_0}\mathbf{K}_{P3,\Omega 1} - s_0\mathbf{M}_{P3,\Omega 1}\right] \end{aligned} \tag{8}$$

and

$$\begin{aligned} \mathbf{C}_{\Omega 2} = \mathbf{M}_{\Omega 2}, \quad \Gamma_{\Omega 2} = -\mathbf{K}_{\Omega 2}, \\ \mathbf{B}_{\Omega 2} = \left[\frac{1}{s_0}\mathbf{K}_{P2,\Omega 2} - s_0\mathbf{M}_{P2,\Omega 2} \quad \frac{1}{s_0}\mathbf{K}_{P3,\Omega 2} - s_0\mathbf{M}_{P3,\Omega 2}\right], \end{aligned} \tag{9}$$

one obtains:

$$\mathbf{B}_{\Omega 1}\left[\begin{array}{c} \mathbf{e}_{P1} \\ \mathbf{e}_{P3} \end{array}\right] = \left(s_0\mathbf{C}_{\Omega 1} + \frac{1}{s_0}\Gamma_{\Omega 1}\right)\mathbf{e}_{\Omega 1} \tag{10}$$

$$\mathbf{B}_{\Omega 2}\left[\begin{array}{c} \mathbf{e}_{P2} \\ \mathbf{e}_{P3} \end{array}\right] = \left(s_0\mathbf{C}_{\Omega 2} + \frac{1}{s_0}\Gamma_{\Omega 2}\right)\mathbf{e}_{\Omega 2}. \tag{11}$$

This form of equations is compliant with the ENOR algorithm. By applying the algorithm to (10) and (11), so that block moments expanded about the selected frequency s_0 are matched [3, 10], one obtains two sets of orthonormal vectors forming two orthonormal bases $\mathbf{V}_{\Omega 1}$ and $\mathbf{V}_{\Omega 2}$. The size of $\mathbf{V}_{\Omega 1}$ and $\mathbf{V}_{\Omega 2}$ is $N_{\Omega 1} \times N_{V1}$ and $N_{\Omega 2} \times N_{V2}$, where N_{V1} and N_{V2} depend on the reduction order q and the number of variables on the appropriate ports [10]:

$$\begin{aligned} N_{V1} &= (N_{P1} + N_{P3})\, q \\ N_{V2} &= (N_{P2} + N_{P3})\, q. \end{aligned} \tag{12}$$

The minimum order of the reduced macro-element is affected mainly by the following factors: the size of the macro-element subdomain, the complexity of the structure embedded in the macro-element and the upper bound of the frequency band. $\mathbf{V}_{\Omega 1}$ and $\mathbf{V}_{\Omega 2}$ can be subsequently applied directly to perform orthogonal projection of the blocks of the FEM Equations (4) that correspond to unknowns in Ω_1, Ω_2. As a result, the reduced system $\mathbf{G}_v \mathbf{e}_v = \mathbf{b}$ is obtained, where:

$$\mathbf{G}_v = \begin{bmatrix} \mathbf{G}_{P1} & 0 & 0 & \mathbf{G}_{P1,\Omega 1}^T \mathbf{V}_{\Omega 1} & 0 \\ 0 & \mathbf{G}_{P2} & 0 & 0 & \mathbf{G}_{P2,\Omega 2}^T \mathbf{V}_{\Omega 2} \\ 0 & 0 & \mathbf{G}_{P3} & \mathbf{G}_{P3,\Omega 1}^T \mathbf{V}_{\Omega 1} & \mathbf{G}_{P3,\Omega 2}^T \mathbf{V}_{\Omega 2} \\ \mathbf{V}_{\Omega 1}^T \mathbf{G}_{P1,\Omega 1} & 0 & \mathbf{V}_{\Omega 1}^T \mathbf{G}_{P3,\Omega 1} & \mathbf{V}_{\Omega 1}^T \mathbf{G}_{\Omega 1} \mathbf{V}_{\Omega 1} & 0 \\ 0 & \mathbf{V}_{\Omega 2}^T \mathbf{G}_{P2,\Omega 2} & \mathbf{V}_{\Omega 2}^T \mathbf{G}_{P3,\Omega 2} & 0 & \mathbf{V}_{\Omega 2}^T \mathbf{G}_{\Omega 2} \mathbf{V}_{\Omega 2} \end{bmatrix} \tag{13}$$

$$\mathbf{e}_v = \begin{bmatrix} \mathbf{e}_{P1} & \mathbf{e}_{P2} & \mathbf{e}_{P3} & \mathbf{e}_{m\Omega 1} & \mathbf{e}_{m\Omega 2} \end{bmatrix}^T$$

and

$$\begin{aligned} \mathbf{e}_{m\Omega 1} &= \mathbf{V}_{\Omega 1}^T \mathbf{e}_{\Omega 1} \\ \mathbf{e}_{m\Omega 2} &= \mathbf{V}_{\Omega 2}^T \mathbf{e}_{\Omega 2}. \end{aligned} \tag{14}$$

Blocks $\mathbf{V}_{\Omega 1}^T \mathbf{G}_{\Omega 1} \mathbf{V}_{\Omega 1}$ and $\mathbf{V}_{\Omega 2}^T \mathbf{G}_{\Omega 2} \mathbf{V}_{\Omega 2}$ of size $N_{V1} \times N_{V1}$ and $N_{V2} \times N_{V2}$ are referred to as macro-element matrices. They are of a much smaller size than $\mathbf{G}_{\Omega 1}$ and $\mathbf{G}_{\Omega 2}$ in the original system, since $N_{V1} \ll N_{\Omega 1}$ and $N_{V2} \ll N_{\Omega 2}$. As a result, the number of variables of the problem is significantly reduced, albeit the macro-element matrices become dense. It should be noted that each macro-element is created independently, so that the reduction process, which is a critical contributor to the overall computational load, can be parallelized. An important advantage is that no additional computations are necessary to perform the parallel reduction of the subdomains. Unlike in [10], where the macro-elements were surrounded by unreduced regions, this formulation allows for reduction in all 3-D subregions that cover the entire structure. The only subdomains of the original problem that remain unchanged are the 2-D ports represented by sparse blocks $\mathbf{G}_{Pk}$ in the system matrix $\mathbf{G}_v$.

In the ENOR algorithm the projection vectors $\mathbf{V}$ are calculated for one arbitrarily chosen frequency s_0 and remain frequency-independent. Thus it is sufficient to perform the reduction only once for very wide frequency range of analysis [3, 10]. This highly attractive property of the $\mathbf{V}$ vectors leads to yet another important advantage of the presented procedure. The reduced system (12) can be reverted to the original form:

$$\left(\mathbf{K}_v - k_0^2 \mathbf{M}_v\right) \mathbf{e}_v = \mathbf{b}, \tag{15}$$

where the reduced FEM matrices $\mathbf{K}_v$, $\mathbf{M}_v$ are calculated in the same way as $\mathbf{G}_v$. Since the matrices $\mathbf{K}_v$ and $\mathbf{M}_v$ remain frequency-independent, the proposed method can also be applied in calculation of the resonant frequencies of the cavities. To this end one sets $\mathbf{b} = 0$ and solves the resulting generalized eigenvalue problem. If one used the segmentation and model order reduction approach adopted in [13], finding the resonances would require solving a nonlinear equation, which is a very time-consuming process.

Post-processing operations (such as computations of far field, input impedance and currents) can be applied to the MOR solution (15). To this end one has to project the field obtained using (15) back onto the original space, using $\mathbf{V}$.

2.3. Modal Projection

The efficiency of the reduction process depends on the following factors: number of variables inside the macro-element subregion, the order of reduction and the number of FEM mesh elements at the interface that couples the macro-element with its surroundings. Whereas the first two factors are implied by the required approximation accuracy of the macro-element, the number of variables at the internal ports (12) should be made as low as possible. Although in 2-D problems it can be limited to less than 10 [10], these numbers are much bigger for 3-D structures, even if aggressive mesh coarsening is used. A large number of variables at macro-element ports in 3-D affects not only the reduction process but also the size of dense submatrices of the reduced macro-elements, eventually leading to deterioration in the efficiency of solving the resulting system.

One of the approaches to overcome this limitation is to apply the projection at the interfaces of the macro-element subdomains before applying the MOR formulation, as postulated in [15] and [24]. For the model problem considered here (Figure 1) the interfaces of the subdomains are the cross-sections of the waveguide denoted as ports P_1, P_2, P_3. The distribution of the tangential electric field at the ports can be expressed as modal expansion based on orthogonal waveguide

TE and TM modes. These modes are used to project the fields at the interfaces prior to creating a macro-element, thereby reducing the number of variables at the interfaces. Although in the case of a simple problem with a uniform rectangular waveguide the modal basis is known analytically and is the same for each port, the proposed procedure does not rely on such limiting assumption. For an arbitrary shape of port that is transversal to the local section of the waveguide, the modal basis is computed at each port separately as a solution of 2-D vector FEM eigenvalue problem [25]. Once N_{Pk} unique eigenvalues and eigenvectors have been calculated, the modal expansion of the tangential electric field is:

$$\mathbf{E}^{(k)} = \sum_{i=1}^{N_{Pk}} a_i^{(k)} \mathbf{e}_{t,i}^{(k)}, \tag{16}$$

where k and i denote port and mode indices, respectively, $a_i^{(k)}$ is the amplitude of the i-th mode and $\mathbf{e}_{t,i}^{(k)}$ is the vector of modal function discretized on a 2-D FEM mesh. If the 2-D mesh at the port conforms to the 3-D mesh in adjacent volumes, the resulting basis can be directly used for modal projection of the fields at macro-elements ports.

In practice, the expansion (16) can be truncated to $\widetilde{N}_{Pk}$ lowest modes without sacrificing the solution accuracy, since higher order modes are heavily attenuated. The required number of modes depends on the extent to which the discontinuities disturb the field distribution in uniform sections of the waveguide. Usually the macro-element ports are sufficiently distanced from the embedded discontinuities and most of high-order modes, called localized [26] vanish before reaching the ports. Only a few modes, called accessible [26], have to be taken into account, thus $\widetilde{N}_{Pk} \ll N_{Pk}$. The required value of $\widetilde{N}_{Pk}$ depends on the field distribution around the discontinuities which is not known a priori. Therefore it can be found by successive evaluation of the structure response for the varying $\widetilde{N}_{Pk}$.

In order to apply the modal projection using the basis consisting of a truncated set of eigensolutions of 2-D problems at internal and external ports, one has to multiply appropriate blocks of matrices in $\mathbf{K}$ (matrix $\mathbf{M}$ is treated in the analogous way) as follows:

$$\widetilde{\mathbf{K}} = \begin{bmatrix} \widetilde{\mathbf{E}}_{P1}^T \mathbf{K}_{P1} \widetilde{\mathbf{E}}_{P1} & 0 & 0 & \widetilde{\mathbf{E}}_{P1}^T \mathbf{K}_{P1,\Omega 1}^T & 0 \\ 0 & \widetilde{\mathbf{E}}_{P2}^T \mathbf{K}_{P2} \widetilde{\mathbf{E}}_{P2} & 0 & 0 & \widetilde{\mathbf{E}}_{P2}^T \mathbf{K}_{P2,\Omega 2}^T \\ 0 & 0 & \widetilde{\mathbf{E}}_{P3}^T \mathbf{K}_{P3} \widetilde{\mathbf{E}}_{P3} & \widetilde{\mathbf{E}}_{P3}^T \mathbf{K}_{P3,\Omega 1}^T & \widetilde{\mathbf{E}}_{P3}^T \mathbf{K}_{P3,\Omega 2}^T \\ \mathbf{K}_{P1,\Omega 1} \widetilde{\mathbf{E}}_{P1} & 0 & \mathbf{K}_{P3,\Omega 1} \widetilde{\mathbf{E}}_{P3} & \mathbf{K}_{\Omega 1} & 0 \\ 0 & \mathbf{K}_{P2,\Omega 2} \widetilde{\mathbf{E}}_{P2} & \mathbf{K}_{P3,\Omega 2} \widetilde{\mathbf{E}}_{P3} & 0 & \mathbf{K}_{\Omega 2} \end{bmatrix}. \tag{17}$$

As a result of modal projection, the unknown FEM coefficients of the basis functions in vectors $\mathbf{e}_{P1}$, $\mathbf{e}_{P2}$ and $\mathbf{e}_{P3}$ are replaced with vectors $\widetilde{\mathbf{e}}_{P1}$, $\widetilde{\mathbf{e}}_{P2}$ and $\widetilde{\mathbf{e}}_{P3}$, each of them comprising $\widetilde{N}_{Pk}$ unknown amplitudes of the waveguide modes $a_i^{(k)}$.

$$\widetilde{\mathbf{e}} = [\widetilde{\mathbf{e}}_{P1} \quad \widetilde{\mathbf{e}}_{P2} \quad \widetilde{\mathbf{e}}_{P3} \quad \mathbf{e}_{\Omega 1} \quad \mathbf{e}_{\Omega 2}]^T \tag{18}$$

Since $\widetilde{N}_{Pk} \ll N_{Pk}$, $k \in \{1, 2, 3\}$, the modal projection significantly reduces the number of unknowns at the ports of macro-elements. The column ranks of orthonormal bases $\mathbf{V}_{\Omega 1}$ and $\mathbf{V}_{\Omega 2}$ as well as the resulting sizes of macro-elements $\widetilde{N}_{V1}$ and $\widetilde{N}_{V2}$ decrease to the same extent:

$$\begin{aligned} \widetilde{N}_{V1} &= \left(\widetilde{N}_{P1} + \widetilde{N}_{P3}\right) q \\ \widetilde{N}_{V2} &= \left(\widetilde{N}_{P2} + \widetilde{N}_{P3}\right) q. \end{aligned} \tag{19}$$

For homogeneous ports, the modal expansion does not introduce frequency-dependent terms, therefore the reduced matrices $\widetilde{\mathbf{K}}$ and $\widetilde{\mathbf{M}}$ remain frequency-invariant.

Without prior knowledge of the response, the minimum order of the model order reduction and the truncation of the modal expansion can be determined by an iterative approach similar to that described in [27]. At each iteration the model order or the expansion order is increased and the response is compared with that obtained in the previous iteration until convergence is achieved. Such a procedure is fast and results in a very small time overhead.

3. NUMERICAL RESULTS

Three 3-D problems are investigated in order to test the performance of the proposed method: a multiple-post filter, a dielectric-loaded filter and a resonator consisting of two coupled dielectric-loaded cavities. All

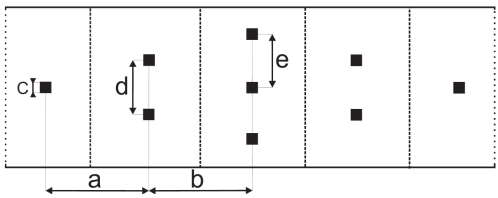

Figure 2. Multiple-post filter. ($a = 10.66\,\text{mm}$, $b = 11.62$, $c = 1\,\text{mm}$, $d = 4.07\,\text{mm}$, $e = 4.71\,\text{mm}$). The internal ports are depicted by the dashed lines, the excitation ports by the dotted lines.

calculations were performed using Matlab on a computer with an Intel i7 processor and 8-GB RAM.

3.1. Example 1: Multiple-post Filter

In the first example the analyzed structure is the WR-62 waveguide (15.799 mm × 7.899 mm) loaded with nine metallic posts of square cross-section (Figure 2). The posts are uniform in the y-direction, which implies that the field does not vary in this direction, so in fact, the structure could be analyzed in 2-D. However, the purpose of this experiment was to examine the validity of the 3-D MOR algorithm, therefore a 3-D formulation was applied. The structure

Table 1. Comparison of the numerical results of the multiple-post filter analysis for the standard FEM and the FEM with macro-elements.

	FEM	FEM with macro-elements
Number of unknowns	362,839	276
Reduction time	-	68 sec
Solution time per freq.	54 sec	0.0036 sec
Solution time for the whole characteristic (73 fp)	66 min	0.262 sec

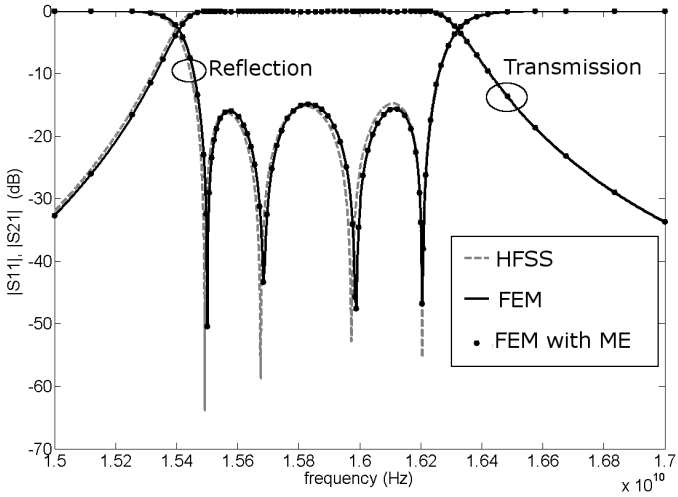

Figure 3. S-parameters of the multiple-post filter simulated using HFSS, standard FEM and FEM with macro-elements.

was discretized using 345,463 tetrahedral elements, which resulted in 362,839 FEM degrees of freedom. First, the standard first-order FEM analysis without macro-elements was carried out in order to generate reference results for further tests concerning effects of model order reduction. The aim of the simulation was to compute the transmission and reflection coefficients over the range of 15 to 17 GHz at 73 frequency points (fp) assuming the TE_{10} mode excitation. The computation time was approximately 54 sec for each frequency point, totaling to 66 min for the whole characteristic (Table 1). The obtained results, shown in Figure 3 are in very good agreement with those computed by means of commercial FEM software Ansys HFSS [28].

Afterwards, the same structure was analyzed by means of the proposed model order reduction algorithm applied to the same mesh and FEM formulation as in the reference analysis. The computational domain was split into five subdomains by placing 4 interfaces in the middle between the groups of metallic posts. This division implies that there are 6 ports of the macro-elements, including 2 excitation ports. Fields at each port were projected onto modal subspaces spanned by first 6 TE waveguide modes. The 4th order of reduction was used, resulting in the size of each macro-element (the number of unknowns) equal to 48. The overall number of unknowns was 276, which is over three orders of magnitude less than in the FEM without macro-elements. The reduction process takes from 11 to 16 sec for each macro-element, depending on the number of discontinuities embedded. After the reduction, the computation time for one fp decreased from 54 sec to as few as 0.0036 sec, which resulted in total 0.262 sec for all 73 fp

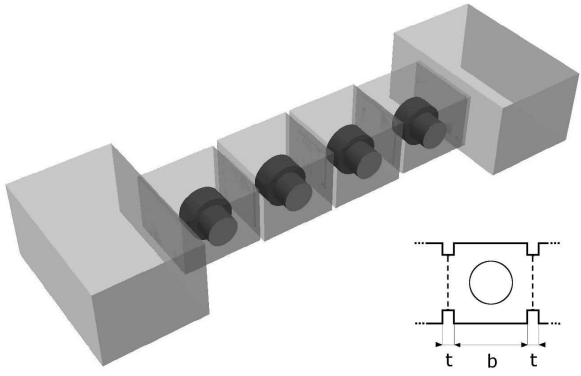

Figure 4. Four-pole dielectric-loaded cavity filter, $t = 0.5$ mm, $b = 9$ mm. All other dimensions are given in [29]. Internal ports for one section of the filter are depicted by the dashed lines in the inset.

(Table 1). The resulting characteristics remain in excellent agreement with the standard FEM formulation over the entire analysis bandwidth (Figure 3). Counting together the total solution time and the reduction time of all 5 macro-elements, the overall speedup is from 66 min to 69 sec, which means the complete calculation was about 57 times faster.

3.2. Example 2: Dielectric-loaded Cavity Filter

For the second example a more complex structure was chosen, namely a four-pole dielectric-loaded cavity filter, shown in Figure 4. The purpose of this test is to demonstrate how the proposed method copes with the structures containing elements that significantly disturb the field distribution. In particular, this test addresses the issue of placing macro-elements near such discontinuities. Four resonators are coupled by rectangular irises and contain large cylindrical dielectric pucks ($\epsilon_r = 30$) on dielectric supports ($\epsilon_r = 9$). The input and output waveguide is WR-75 (19.05 mm × 9.52 mm). All other dimensions of the filter are given in [29].

As in the first example, in order to generate reference results, the filter was analyzed by means of the standard FEM formulation, using 798,175 degrees of freedom. Such a large problem resulted from strong local mesh refinement required in big volumes, which was caused by the presence of very high permittivity dielectric cylinders of relatively large diameter. The scattering parameters of the filter were computed

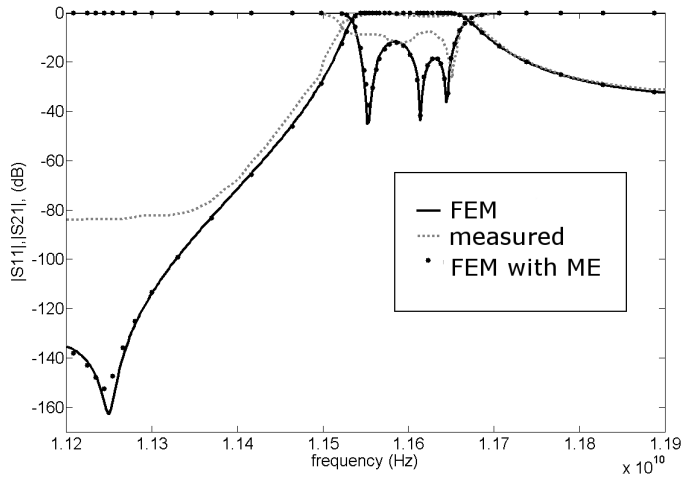

Figure 5. S-parameters of the dielectric-loaded resonator filter simulated using standard FEM, FEM with macro-elements and compared to the measurements [29].

Table 2. Comparison of the performance of the dielectric-loaded cavity filter analysis for the standard FEM and the proposed algorithm of FEM with macro-elements.

	Standard FEM	FEM with macro-elements
Number of unknowns	798,175	550
Reduction time	-	570 sec
Simulation time per freq.	6–8 min	0.0144 sec
Simulation time for the whole characteristic in 55 fp	400 min	0.79 sec

at 55 fp covering the bandwidth of 11 to 12 GHz. Good agreement with experimental results reported in [29] is achieved, as shown in Figure 5. The computation time for one frequency is approximately 6–8 min, which results in about 400 min for the whole frequency response.

Upon setting the reference results, the filter was analyzed using the proposed method. Five internal ports were placed in the middle of rectangular coupling irises. This partitioning gives 6 subdomains-all subject to the model order reduction, which turns them into 6 macro-elements. The dominant source of field disturbances in the structure are the dielectric cylinders. Since they excite higher modes closer to macro-element ports than in the first example, longer modal expansion is required. The first 10 waveguide modes were experimentally selected for modal projection and found to provide sufficient accuracy of approximation while at the same time yield radical decrease in the number of unknowns at the ports. With the reduction order $q = 4$, the overall number of unknowns in the whole domain decreases from 798,175 to just 550. The reduction process for each of the macro-elements takes from 54 to 102 sec. The solution of the reduced system and computation of the scattering parameters takes 0.0144 sec per each frequency and 0.792 sec for the whole characteristic (55 fp). As in the first example, one can observe very good agreement between the results obtained in the standard FEM and FEM with macro-elements. The comparison of the problem size and computation time for these two methods is presented in Table 2. Even though the computation time is dominated by the time of reduction (54 sec to 102 sec per one ME), the overall speedup for the whole 55 point frequency response is from 400 min to 570 sec, which is an impressive number of 42 times.

3.3. Example 3: Dielectric-loaded Resonator

The purpose of the last example is to illustrate the capability of the proposed method to solve eigenvalue problems in resonant frequency

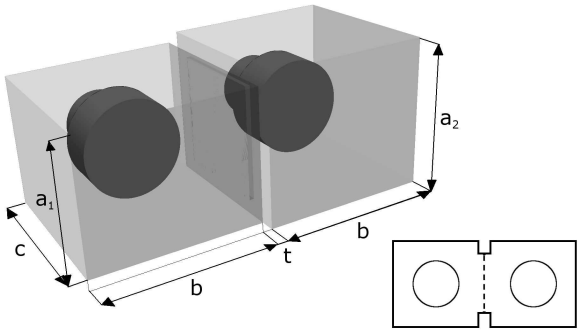

Figure 6. Two-cavity dielectric-loaded resonator based on the filter presented in Figure 4, $a_1 = 6.91\,\text{mm}$, $a_2 = 7.93\,\text{mm}$, $b = c = 9\,\text{mm}$ and $t = 0.5\,\text{mm}$. Other parameters are identical as for the structure in Figure 4. The internal port is depicted by the dashed line.

Table 3. Comparison of the numerical results of the dielectric-loaded resonator analysis for the standard FEM, FEM with macro-elements and HFSS.

HFSS Results (GHz)	FEM without ME (GHz)	FEM with ME (GHz)	Error (%) HFSS/FEM	Error (%) FEM/FEM-ME
11.6857	11.6303	11.6303	0.47	0.0065
11.8817	11.8316	11.8316	0.42	0.0007

calculations. The analyzed structure is a resonator created from two coupled cavities, as in the previous example. The geometry is detailed in Figure 6. The discretization of the structure results in 218,283 FEM degrees of freedom. For the generalized eigenvalue problem and the standard FEM formulation, which serves as a reference for the proposed method, it takes 842 sec to compute the first two resonant frequencies by means of the Implicitly Restarted Arnoldi Method (IRAM).

The domain partitioning for applying the FEM with MOR is accomplished by placing one interface in the middle of the coupling iris between the two cavities, as in the previous example, which creates two macro-elements. A satisfying agreement with the reference results (Table 3) requires projecting the field at the interface onto a modal subspace spanned by the first 11 waveguide modes and setting the order of reduction in the two subdomains to $q = 6$. These numbers are slightly bigger than in the filter example. It can be attributed to the fact that for eigenvalue problems better approximation is

needed, as here the field distribution is not constrained by fundamental mode excitation present in driven problems. The total number of unknowns of the resulting system is 143 and the reduction times for the subdomains are 42.4 and 64.1 sec. The same eigensolver (IRAM) was used for the reduced problem and the solution time proved to be as short as 0,044 sec. To assess the overall efficiency of the FEM with macro-elements the reduction time has to be taken into account, but nonetheless the total speedup is as much as about 8 times. The resonator was also simulated using the HFSS to validate the results obtained with the presented method. The results are compared in Table 3. It was observed that the error introduced by the reduction was practically negligible. The results from standard FEM, as well as those from the proposed MOR method, agree with the HFSS results. The occurrence of small error of less than 0.5% can be attributed to better FEM approximation in HFSS, in which higher-order curvilinear elements and adaptive mesh refinement are employed.

4. CONCLUSION

An efficient model order reduction method for three-dimensional FEM analysis of waveguide structures has been proposed. The computational domain is divided into cascaded subdomains, in which model order reduction is performed locally by means of the ENOR algorithm. The resulting macro-elements are represented by submatrices of significantly reduced size, which allows for faster solution of the underlying system of equations. In order to additionally improve the effectiveness of the proposed method, fields at macro-element interfaces are projected onto a modal subspace spanned by a few low-order waveguide modes. Thus, by decreasing the number of unknowns at macro-element ports, the reduction itself is considerably accelerated and the resulting matrices become even more compressed. An additional advantage of the presented method is that the reduced-order system matrix is frequency-independent, which allows for very fast frequency sweeping and efficient calculation of resonant frequencies without the need of nonlinear eigensolvers. Several numerical examples for driven and eigenvalue problems have demonstrated very good performance of the proposed methodology in terms of accuracy, memory usage and simulation time.

ACKNOWLEDGMENT

The authors would like to thank Dr. A. Lamecki for providing a simplified Matlab version of the finite element code which was used

in the research reported in this paper and Dr. L. Kulas for his valuable assistance and providing the Matlab code of the ENOR algorithm. This work has been financed by MNiSzW under grant 5407/B/T02/2010/38.

REFERENCES

1. Celik, M. and A. C. Cangellaris, "Simulation of dispersive multiconductor transmission lines by Padé approximation via the Lanczos process," *IEEE Trans. Microwave Theory Tech.*, Vol. 44, 2525–2535, Dec. 1996.
2. Odabasioglu, A., M. Celik, and L. T. Pileggi, "PRIMA: Passive reduced order interconnect macromodeling algorithm," *IEEE Trans. Computer-Aided Design*, Vol. 17, 645–653, Aug. 1998.
3. Sheehan, B. N., "ENOR: Model order reduction of RLC circuits using nodal equations for efficient factorization," *Proc. IEEE 36th Design Autom. Conf.*, 17–21, Jun. 1999.
4. Rewienski, M. and J. White, "A trajectory piecewise-linear approach to model order reduction and fast simulation of nonlinear circuits and micromachined devices," *IEEE Transactions on Computer-Aided Design of Integrated Circuits and Systems*, Vol. 22, No. 2, 155–170, Feb. 2003.
5. Cangellaris, A. C., M. Celik, S. Pasha, and L. Zhao, "Electromagnetic model order reduction for system-level modeling," *IEEE Trans. Microwave Theory Tech.*, Vol. 7, 840–850, Jun. 1999.
6. Denecker, B., F. Olyslager, L. Knockaert, and D. De Zutter, "Automatic generation of subdomain models in 2-D FDTD using reduced order modeling," *IEEE Microwave Guided Wave Lett.*, Vol. 10, 301–303, Aug. 2000.
7. Kulas, L. and M. Mrozowski, "Reduced-order models in FDTD," *IEEE Microw. Wireless Comp. Lett.*, Vol. 11, No. 10, 422–424, Oct. 2001.
8. Kulas, L. and M. Mrozowski, "Reduced order models of refined Yee's cells," *IEEE Microw. Wireless Comp. Lett.*, Vol. 13, 164–166, Apr. 2003.
9. Zhu, Y. and A. C. Cangellaris, "Macro-elements for efficient FEM simulation of small geometric features in waveguide components," *IEEE Trans. Microwave Theory Tech.*, Vol. 48, 2254–2260, Dec. 2000.
10. Fotyga, G., K. Nyka, and L. Kulas, "A new type of macro-elements for efficient two-dimensional FEM analysis," *IEEE Antennas and Wireless Propagation Letters*, Vol. 10, 270–273, 2011.

11. Lee, S.-H. and J. M. Jin, "Fast reduced-order finite-element modeling of lossy thin wires using lumped impedance elements," *IEEE Trans. Adv. Packag.*, Vol. 33, No. 1, 212–218, Feb. 2010.
12. Kulas, L. and M. Mrozowski, "Accelerated analysis of resonators by a combined domain decomposition — Model order reduction approach," *34th European Microwave Conference*, Vol. 2, 585–588, Oct. 14, 2004.
13. De la Rubia, V. and J. Zapata, "Microwave circuit design by means of direct decomposition in the finite-element method," *IEEE Trans. Microwave Theory Tech.*, Vol. 55, No. 7, 1520–1530, Jul. 2007.
14. Kulas, L. and M. Mrozowski, "Macromodels in the frequency domain analysis of microwave resonators," *IEEE Microw. Wireless Comp. Lett.*, Vol. 14, No. 3, 94–96, Mar. 2004.
15. Kulas, L., P. Kowalczyk, and M. Mrozowski, "A novel modal technique for time and frequency domain analysis of waveguide components," *IEEE Microw. Wireless Comp. Lett.*, Vol. 21, No. 1, 7–9, Jan. 2011.
16. Remis, R. F., "An efficient model-order reduction approach to low-frequency transmission line modeling," *Progress In Electromagnetics Research*, Vol. 101, 139–155, 2010.
17. Zhang, Z. and Y. H. Lee, "An automatic model order reduction of a UWB antenna system," *Progress In Electromagnetics Research*, Vol. 104, 267–282, 2010.
18. Song, Z., D. Su, F. Duval, and A. Louis, "Model order reduction for PEEC modeling based on moment matching," *Progress In Electromagnetics Research*, Vol. 114, 285–299, 2011.
19. Rubio, J., J. Arroyo, and J. Zapata, "Analysis of passive microwave circuits by using hybrid 2-D and 3-D finite-element mode-matching method," *IEEE Trans. Microwave Theory Tech.*, Vol. 47, No. 9, 1746–1749, Sep. 1999.
20. Mrozowski, M., "A hybrid PEE-FDTD algorithm for accelerated time domain analysis of electromagnetic waves in shielded structures," *IEEE Microwave Guided Wave Lett.*, Vol. 4, No. 10, 323–325, Oct. 1994.
21. Jin, J. M., *The Finite Element Method in Electromagnetics*, 2nd edition, IEEE Press, New York, 2002.
22. Pelosi, G., R. Coccioli, and S. Selleri, *Quick Finite Elements for Electromagnetic Waves*, 2nd Edition, Artech House Antenna Library, 2009.

23. Ingelstrom, P., "A new set of H(curl)-conforming hierarchical basis functions for tetrahedral meshes," *IEEE Trans. Microwave Theory Tech.*, Vol. 54, No. 1, 106–114, Jan. 2006.
24. Kowalczyk, P., L. Kulas, and M. Mrozowski, "Analysis of microstructured optical fibers using compact macromodels," *Opt. Express*, Vol. 19, No. 20, 19354–19364, 2011.
25. Lou, Z. and J. M. Jin, "An accurate waveguide port boundary condition for the time-domain finite-element method," *IEEE Trans. Microwave Theory Tech.*, Vol. 53, No. 9, 3014–3023, Sep. 2005.
26. Stamatopoulos, I. D. and I. D. Robertson, "Rigorous network representation of microwave components by the use of indirect mode matching," *IEEE Trans. Microwave Theory Tech.*, Vol. 52, No. 3, 935–944, Mar. 2004.
27. Zhu, Y. and A. C. Cangellaris, *Multigrid Finite Element Methods for Electromagnetic Field Modeling*, Wiley, New York, 2006.
28. ANSYS HFSS, "3D full-wave electromagnetic field simulation," http://www.anasoft.com/products/hf/hfss/overview.cfm.
29. Alessandri, F., M. Chiodetti, A. Giugliarelli, D. Maiarelli, G. Martirano, D. Schmitt, L. Vanni, and F. Vitulli, "The electric field integral-equation method for the analysis and design of a class of rectangular cavity filters loaded by dielectric and metallic cylindrical pucks," *IEEE Trans. Microwave Theory Tech.*, Vol. 52, No. 8, 1790–1797, Aug. 2004.